JACS
JOURNAL OF THE AMERICAN CHEMICAL SOCIETY
Article
pubs.acs.org/JACS

Role of Organic Solvents in Immobilizing Fungus Laccase on Single-Walled Carbon Nanotubes for Improved Current Response in Direct Bioelectrocatalysis

Fei Wu,[†,‡,§] Lei Su,[†,§] Ping Yu,[†,‡] and Lanqun Mao*[,†,‡]

[†]Beijing National Laboratory for Molecular Science, Key Laboratory of Analytical Chemistry for Living Biosystems, Institute of Chemistry, the Chinese Academy of Sciences, Beijing 100190, China

[‡]University of Chinese Academy of Sciences, Beijing 100049, China

Supporting Information

ABSTRACT: Improving bioelectrocatalytic current response of redox enzymes on electrodes has been a focus in the development of enzymatic biosensors and biofuel cells. Herein a mediatorless electroreduction of oxygen is effectively improved in terms of a remarkable enhancement by ca. 600% in maximum reductive current by simply adding 20% ethanol into laccase solution during its immobilization onto single-walled carbon nanotubes (SWCNTs). Conformation analysis by circular dichroism and attenuated total reflectance infrared spectroscopy demonstrate promoted laccase-SWCNTs contact by ethanol, thus leading to favorable enzyme orientation on SWCNTs. Extended investigation on acetone-, acetonitrile-, *N*,*N*-dimethylformamide (DMF)-, or dimethyl sulfoxide (DMSO)-treated laccase-SWCNTs electrodes shows a 400% and 350% current enhancement at maxima upon acetone and acetonitrile treatment, respectively, and a complete diminish of reductive current by DMF and DMSO. These results together reveal the important role of organic solvents in regulating laccase immobilization for direct bioelectrocatalysis by balancing surface wetting and protein denaturing.

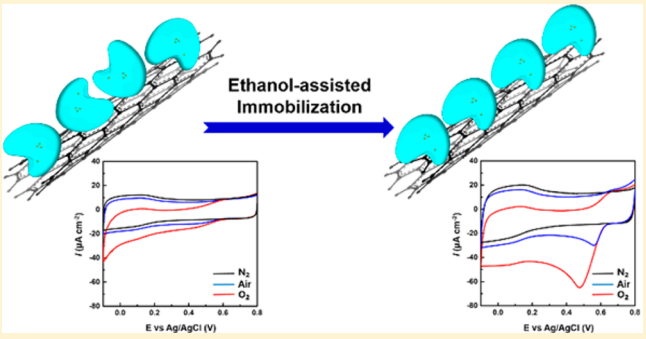

INTRODUCTION

In the realm of biofuel cells and biosensing, laccase has received enormous attention for its catalytic ability in bioelectroreduction of oxygen. Being one of the blue multicopper oxidases (MCOs), laccase comprises totally four copper atoms classified into a mononuclear type-1 (T1) copper abstracting electrons from phenolic substrates, and a trinuclear type-2 (T2)/type-3 (T3) copper cluster reducing oxygen to water. A highly conserved histidine-cysteine-histidine tripeptide bridges T1 copper and T2/T3 cluster as an intramolecular electron transfer (IET) highway.[1] Compared to precious metallic catalysts, laccase possesses unique advantages, such as high catalytic efficiency at high redox potentials, clean oxygen reduction avoiding peroxide toxicification, resistance to contamination and relatively low cost. In spite of these superiorities, heterogeneous electron transfer through the insulating protein matrix and interfacial space remains a major challenge in designing enzymatic electrodes for improved bioelectrocatalytic current response. Common strategies can be divided into two aspects: mediated electron transfer (MET) and direct electron transfer (DET). The former strategy involves incorporation of redox mediators to shuttle electrons between laccase active sites and electrodes, and current densities have been greatly enhanced as reported.[2] MET-based systems, however, are frequently concomitant with overpotential increase, voltage output drop and mediator leaching. Therefore, DET via fast interfacial tunneling has emerged as a central theme of research on mediator-free bioelectrocatalysis for miniaturized, integratable or implantable bioelectronic devices.

Efficient direct electroreduction of oxygen relies on a close proximity (within 1.5 nm) of the laccase copper sites to the electrode surface.[3,4] X-ray crystallography has shown that a monomeric laccase from fungus or plants consists of three domains (D1, D2, D3) which together constitute an antiparallel β-sheet barrel with a hydrophobic interior. Primary electron acceptor (T1 copper) sits about 6.5 Å underneath the protein surface in D3, while T2/T3 copper cluster is about 12 Å deeply embedded between D1 and D3 (Figure 1).[1] Accordingly, DET between T1 copper and electrodes is readily achievable with favorable positioning of the hydrophobic binding pocket at electrode surfaces. Ever since the first DET example of laccase absorbed on a carbon black electrode reported in 1978,[5] a main body of the efforts have focused on engineering the electrode-enzyme interface aimed at rational immobilization. These include physical adsorption on planar or nanostructred carbonaceous or gold electrodes,[5−20] conductive wiring by

Received: November 4, 2016
Published: January 4, 2017

DOI: 10.1021/jacs.6b11469
J. Am. Chem. Soc. 2017, 139, 1565−1574

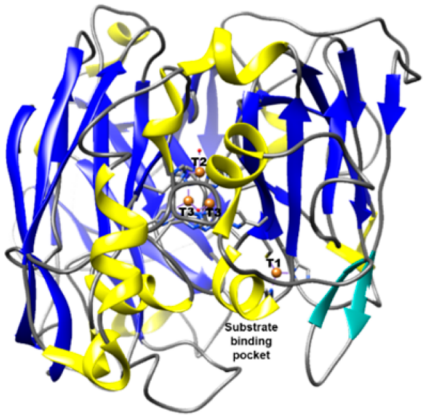

Figure 1. Crystal structure of fungus laccase from *Trametes versicolor* (PDB 1GYC) with its secondary structures highlighted. Blue: antiparallel β-strands. Yellow: α-helices. Dark gray: unordered structures including random coils and turns. Cyan: extended β-strand. Orange spheres represent copper ions. Small red spheres represent bound hydroxo ligands. Thin sticks represent the coordination sites.

carbon nanotubes (CNTs), carbon or gold nanoparticles,[21−31] entrapment in polymers, liquid-crystal cubic phases, carbon microcrystals or aerogels,[32−38] covalent conjugation by cross-linkers, pyrene derivatives or self-assembled thiol monolayers,[30,39−48] supramolecular wiring by substrate-mimicking ligands,[49−58] and site-directed tethering by non-natural amino acids or affinity tags.[59,60] Another important aspect of improving DET calls for reduction of the protein backbone. For example, a part of the peptide chain hindering T1 copper can be genetically removed to increase DET rate with the truncated laccase.[61] Small bacterial laccase (SLAC) has also be introduced into DET construction due to naturally lessened spatial hindrance as well as mising glycosylated shell.[62,63]

Among all nanomaterials for laccase immobilization, CNTs have attracted particular concerns because of their excellent conductivity, robustness and high surface area. Our group reported the first success in DET of laccase physically adsorbed on single-walled CNTs (SWCNTs) and cellulose derivative-modified multiwalled CNTs (MWCNTs) a decade ago.[21,22] Soon later Bilewicz et al. provided a series of nanostructured platforms incorporated with CNTs to build direct electrical connectivity for laccase.[20] Dong et al. introduced a layer-by-layer fabrication of the laccase/poly-$_L$-lysine/CNT composites capable of direct bioelectrocatalysis.[25] Barton et al. realized DET-based oxygen reduction by entrapping SLAC in a SWCNT-containing Nafion film.[62] High current/power densities of oxygen-consuming biofuel cells were achieved through controlled immobilization of laccase in a free-standing film of CNT forest by Nishizawa et al.,[64] and through mechanical compression of laccase into a pure CNT disk by Cosnier et al.[65] With pyrene-succinimidyl ester-modified MWCNTs, Ramasamy et al. were able to study DET kinetics in covalently conjugated laccase during oxygen reduction.[66] Taking advantage of the hydrophobic binding pocket in laccase, supramolecular wiring opens up a unique road toward DET on tailored CNTs. Minteer et al. developed a synthetic linker bearing an anthracene head and a pyrene tail to wire the active site of laccase by aromatic docking.[45,53] Bilewicz et al. further thoroughly explored effects of phenyl, naphthyl, terphenyl, anthracene and anthraquinone wires in directing laccase molecules on arylated CNTs.[56,57] Similar attempt was made by Cosnier et al. using adamantine-modified MWCNTs to rationalize laccase orientation.[55]

Direct bioelectrocatalysis by laccase adsorbed on CNTs has been ascribed to controlled enzyme orientation through hydrophobic and $\pi-\pi$ interactions between the CNT surface and aliphatic and aromatic residues inside the substrate-binding pocket.[67] Even so, ideal positioning of laccase on CNTs without external driving forces is difficult to achieve, in particular concerning the narrow pocket opening (~1 nm), glycosylated and hydrated shell against hydrophobic surface interactions, and discrete nonpolar patches on the protein surface that may yield different molecular orientations. Besides supramolecular aromatic wiring as mentioned above, enzyme inhibitors including organic solvents might help orientate laccase molecules on CNTs. So far, quite a number of CNT-based laccase electrodes featuring DET, especially those requiring Nafion entrapment, have been prepared from aqueous-nonaqueous mixtures,[33,34,68] and it was reported recently that laccase adsorbed from an ethanol-buffer solution onto MWCNT-covered carbon paste electrodes gave larger current densities.[19] However, potential effects of organic solvents on laccase immobilization and subsequent bioelectrocatalytic performance have never been analyzed. Starting from this point, we embarked on the simple immobilization approach by adsorbing laccase onto SWCNTs with a moderate content of ethanol in buffered solution. Voltammetric characterization illustrated a significant enhancement in direct reduction current with the laccase-SWCNT-modified electrode prepared from an ethanol−water mixture. To better understand the role of ethanol during laccase immobilization, circular dichroism and infrared spectroscopy were used to elucidate the conformation and orientation changes of laccase upon physical adsorption. Furthermore, a series of common organic solvents were examined to gain an insight into the relation between their physiochemical properties and direct bioelectrocatalysis.

EXPERIMENTAL SECTION

Preparation of Laccase-SWCNT Electrodes. Crude laccase powder obtained from *Trametes versicolor* (1 g, Sigma-Aldrich) was initially cleaned up as previously described.[22] Chromatographically pure laccase for spectroscopic experiments was prepared as follows: crude powder was dissolved in 10 mL of 0.01 M sodium acetate (pH 6.0) and filtered through a 0.20 μm syringe filter unit. Proteins were then precipitated by ammonium sulfate at 80% of its saturation for 12 h at 4 °C under gentle stirring. Precipitates were collected at 12000 g for 20 min and redissolved in 2.5 mL of 0.01 M sodium acetate buffer (pH 6.0). Resultant solution was quickly desalted through a PD-10 Sephadex G25 column (GE Healthcare), followed by anion-exchange separation through a Q-Sepharose Fast Flow (GE Healthcare) column eluted by step-washing (0.01 M, 0.02 M, 0.05 M, 0.10 and 0.20 M sodium acetate, pH 6.0). Collected fractions exhibiting laccase activities toward ABTS were pooled in an Amicon filter unit (mass cutoff: 10 kDa) at 5000 g. Purified blue laccase was then verified by SDS-PAGE (Figure S1) and UV−vis spectroscopy (Figure S2). Protein concentration was determined by BCA assay.

Glassy carbon electrodes (GCE, diameter: 3 mm, CHI Instruments) were prepolished with alumina slurry (0.3 and 0.05 μm) on a polishing cloth and cleaned by sonication in ethanol and deionized water. SWCNTs (purity: >90%, diameter: 1−2 nm, length: 5−30 μm, purchased from Beijing DK Nano Technology Co. LTD) were purified by refluxing in 2.6 M nitric acid for 10 h. Purified SWCNTs were then dispersed in 50% ethanol under sonication for 15 min to get a uniform suspension (2 mg mL^{-1}), 5 μL of which was coated onto each GCE by drop-casting and dried under a hot incandescent lamp for 1 h. Equal volumes of laccase solution and SWCNT suspension (in deionized water) were mixed on vortex in the absence or presence of 20%

DOI: 10.1021/jacs.6b11469
J. Am. Chem. Soc. 2017, 139, 1565−1574

ethanol, acetonitrile, acetone, DMF or DMSO for 1 min and then by sonication for 1 min at room temperature. After that, another 5 μL of the laccase-SWCNT mixture was pipetted onto the SWCNT-modified GCE. All electrodes were slowly dried under ambient air at room temperature for 2 h in an inverted beaker to allow sufficient contact between laccase molecules and the SWCNT surface.

Electrochemical Evaluation of Direct Bioelectrocatalysis. Cyclic voltammetry of as-prepared electrodes was conducted in a three-electrode system linked to a CHI potentiostat. A platinum spiral wire and an Ag/AgCl electrode (KCl-saturated) were used as counter electrode and reference electrode, respectively. Sodium phosphate buffer or sodium acetate buffer (0.10 M, pH 6.0) was used as the medium and supporting electrolyte. N_2- or O_2-saturated solution was prepared by purging with high-purity N_2 or O_2 gas for at least 30 min before test. CV scanning setup was as follows: 0.8 to −0.1 V, 10 mV sec^{-1}, 2 cycles.

Conformation Analysis by Circular Dichroism. Purified laccase (1 mg mL^{-1}) was incubated with or without SWCNTs in the absence or presence of 20% ethanol in 0.050 M sodium acetate buffer (pH 6.0) under gentle agitation for 15 min at room temperature. Circular dichroism (CD) spectra were collected with a demountable cuvette (light path: 0.02 cm) in a JASCO circular dichroism spectrometer (J-815). CD scanning setup was as follows: 260 nm −180 nm, 200 nm/min, 0.25 s response (time constant), 1 nm bandwidth. Blank solutions containing no laccase were scanned as baselines. All spectra were averaged from five repeats. Spectra analysis according to existed reference set[69] was accomplished by the *DichroWeb* server at http://dichroweb.cryst.bbk.ac.uk/html/home.shtml.[70−72] Mean residual ellipticity was calculated using a molecular weight of *Trametes versicolor* laccase being 56 kDa and residue number being 499.

Conformation Analysis by Infrared Spectroscopy and Spectra Processing. For attenuated total reflectance infrared spectroscopic (ATR-IR) measurements, 5 μL of the laccase-SWCNT mixture was dropped onto a CaF_2 slide, which was dried under ambient air at room temperature for 2 h in a half-covered Petri dish and then in vacuum overnight. Dried laccase-SWCNT films were analyzed by a Fourier Transform (FT) IR spectrophotometer equipped with an ATR accessory. Different IR spectra were obtained by subtracting a reference spectrum collected with the bare SWCNT film after a nine-point smoothing of raw spectra. Second- and fourth-derivative IR spectra were obtained using a five-point Savitsky-Golay function. All spectra processing and peak measurements were done in *OMNIC*. To assess the secondary structures in laccase, curve fitting of the amide I band was conducted in *Origin* to derive Gaussian component bands by the following procedure. Briefly, a linear baseline was drawn between 1700 and 1600 cm^{-1} on the difference IR spectrum without subtraction. Band width was initially set to 8 cm^{-1}. Peak positions assigned according to second-/fourth-derivative IR spectra and literature were allowed to shift slightly during fitting.

RESULTS AND DISCUSSION

Synthetic substrate analogues carrying aromatic moieties were designed to wire laccase molecules on surfaces through $\pi-\pi$ interactions, the rationale for immobilization by supramolecular docking.[45,51,53,55−57] Following this idea, another potential solution to laccase orientation control may be provided by enzyme inhibitors that can occupy the binding pocket and reside on surfaces of CNTs as well. In the work by Haber et al., a list of water-miscible organic solvents were identified as laccase inhibitors.[73,74] In the meantime, many of these organic inhibitors exhibit different affinities to the conjugated surface of CNTs according to solvent nature.[75] Therefore, this work was originated from the question: can organic solvent molecules affinitive to both the substrate binding sites and the CNT surface, similar to anthracene-pyrene linkers, help control the immobilization orientation of laccase on CNTs? To address our concern, ethanol, the most commonly used organic solvent in lab and a laccase inhibitor as well, was chosen as the model cosolvent introduced into the laccase-SWCNT mixture to assist immobilization.

Effect of Ethanol on Direct Reduction Current Response of Laccase on SWCNTs. Figure 2 presents

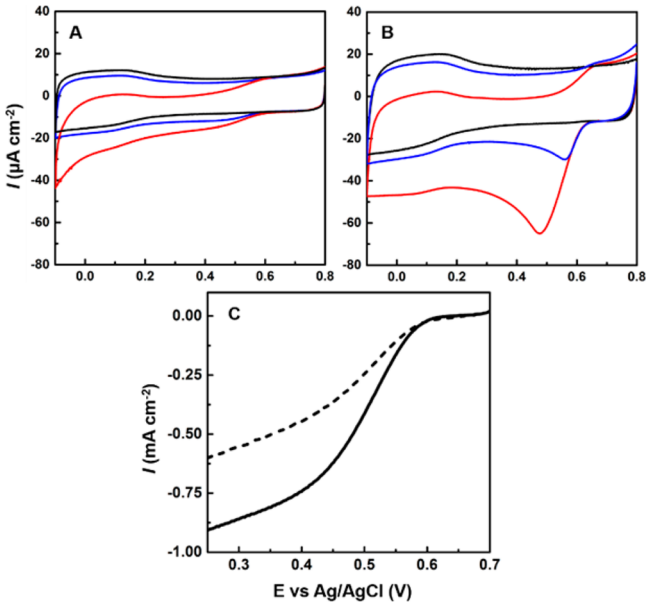

Figure 2. Direct electroreduction of O_2 catalyzed by laccase. Top: Cyclic voltammograms of untreated laccase (A) or ethanol-treated laccase (B) immobilized on SWCNT/GCE in N_2-saturated (black line), air-saturated (blue line) and O_2-saturated (red line) sodium phosphate buffer (0.1 M, pH 6.0). Scan rate, 10 mV sec^{-1}. Bottom: (C) linear sweep voltammograms of untreated laccase (dashed line) or ethanol-treated laccase (solid line) immobilized on SWCNT-modified rotating ring disk electrodes in O_2-saturated phosphate buffer. Scan rate, 10 mV sec^{-1}. Rotating speed, 500 rpm.

representative cyclic voltammograms of the untreated or ethanol-treated laccase-SWCNTs electrodes in 0.1 M phosphate buffer (pH 6.0). Cathodic currents in oxygenated solutions starting at ca. + 0.60 V (vs. Ag/AgCl) close to the formal reduction potential of fungus laccase (+0.78 V vs NHE)[76] confirmed the bioelectrocatalytic activity of laccase-SWCNT composites toward oxygen reduction without mediators, which was also evidenced by the disappearance of turnover currents in deoxygenated solutions. Switching from untreated laccase-SWCNT to ethanol-treated laccase-SWCNT composites only caused a small positive shift in open circuit potential as well as onset potential for oxygen reduction by ca. 15 mV as shown by polarization curves (Figure S3), but resulted in marked changes in current response. The ethanol-treated laccase-SWCNT electrode displayed a steep reductive peak with its maximum current density being 16.6 μA cm^{-2} at +0.56 V under ambient air and 50.9 μA cm^{-2} in oxygen-saturated solution at +0.47 V (all background subtracted). Contrarily, the oxygen reduction current at the untreated laccase-SWCNT electrode was significantly reduced and almost reached a plateau at +0.45 V (2.7 μA cm^{-2}) under ambient air and at +0.35 V (7.3 μA cm^{-2}) under oxygen saturation. To exclude oxygen diffusion limitation, hydrodynamic examination at a rotation speed of 500 rpm was conducted on rotating disk electrodes (RDEs) modified by laccase-SWCNT composites. As shown in Figure 2C, oxygen reduction at the ethanol-treated laccase-SWCNT RDE yielded a current density of 711 μA cm^{-2}

DOI: 10.1021/jacs.6b11469
J. Am. Chem. Soc. 2017, 139, 1565−1574

at +0.4 V, which increased by about 70% from that obtained with the untreated laccase-SWCNT RDE (415 μA cm^{-2}).

We then investigated electron transfer pathways at the electrode-laccase interface through halide inhibiting experiments. *Trametes versicolor* laccase purified from oxygenated solutions was in its resting oxidized form with a hydroxo ligand bridging T3 coppers (proved by UV−vis absorbance at 330 nm resulted from μ_2−OH to T3 copper charge transfer transition, Figure S2).[77] During the voltammetric scan from 0.8 to 0.0 V under anaerobic condition, laccase could undergo a relatively slow four-electron transition from the resting oxidized form to the fully reduced form, which was accomplished by DET from the electrode to T1 copper and subsequent IET to T2 copper.[77] This corresponds to the cathodic peak (Cu^{2+}/Cu^{1+}) at ca. + 0.45 V in N_2-saturated solution that was 400% higher at the ethanol-treated laccase-SWCNT electrode (5.28 μA/cm^{-2}, Figure 3B) than at the untreated laccase-SWCNT electrode

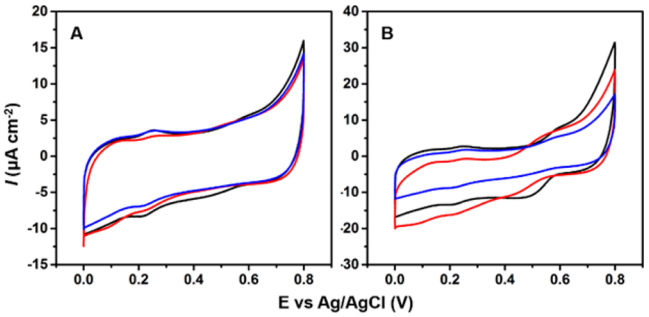

Figure 3. Cyclic voltammograms of untreated laccase (A) or ethanol-treated laccase (B) on SWCNT/GCE in N_2-saturated sodium acetate buffer (0.1 M, pH 6.0) in the absence (black line) or presence of inhibiting ions: 150 mM NaCl (red line); 1 mM NaF (blue line). Scan rate, 5 mV sec^{-1}.

(0.88 μA/cm^{-2}, Figure 3A). As controls, no redox peaks were obtained with either untreated or ethanol-treated laccase immobilized on planar GCEs (Figure S4), showing the essential role of SWCNTs in connecting the electrode and laccase coppers. In the presence of 150 mM Cl^-, which was previously suggested to coordinate T1 copper as a competitive inhibitor,[42,78,79] maximum reductive current at +0.45 V was reduced by 63% for untreated laccase-SWCNTs while only 26% for ethanol-treated laccase-SWCNTs. It is in good agreement with the published finding that Cl^- has less inhibitory effect on laccase molecules in an appropriate orientation with the substrate binding pocket facing the electrode surface due to potential steric hindrance to Cl^- access to T1 copper,[58,78−80] even though we are still not clear about the reason for the decrease of nonturnover current of Cl^--coordinated T1 copper. Interestingly, reductive current of ethanol-treated laccase-SWCNTs at +0.40 V did not change (4.77 μA/cm^{-2}) upon blockade of T1 copper by Cl^- and even increased after NaCl addition as scanned more negatively, which was not observed for untreated laccase-SWCNTs. Contrarily, similar current suppression was observed for both types of electrodes when 1 mM NaF was added to strongly inhibit T2 copper and shut down T1-T2/T3 IET, resulting in almost complete loss of the electrochemical activity of laccase. Taken together, inhibition data imply one plausible possibility of the current contribution from the electrode-T2/T3 copper cluster DET in ethanol-treated laccase-SWCNT composites that was not influenced by Cl^- but blocked by F^-. Small cathodic peaks were spotted at ca. +0.20 V and appeared to be independent of halide coordination (no significant changes in either potential or current density), which were most likely due to impurities or even dissociated coppers.

Effect of Ethanol on Laccase Conformation. Conformational changes of laccase during physical adsorption before dehydration were characterized by circular dichroism. Far-UV spectra of chromatographically purified laccase in different solutions were collected to analyze protein secondary structures (Figure 4, top). The positive peak at 198 nm and negative peak

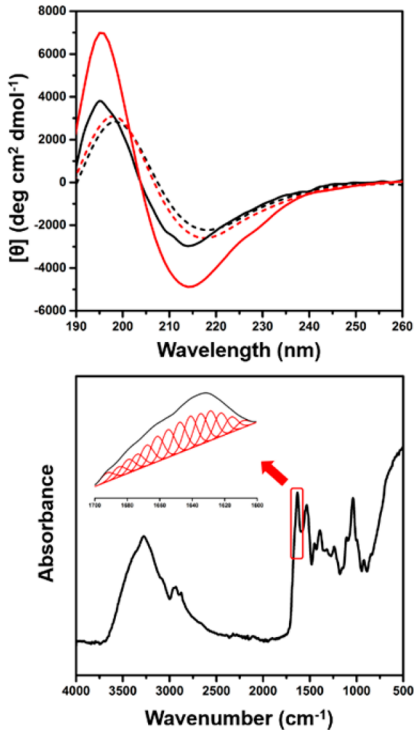

Figure 4. Spectroscopic elucidation of the laccase conformation. Top: Far-UV CD of untreated laccase (black line) or ethanol-treated laccase (red line) in sodium acetate buffer (0.05 M, pH 6.0) with (solid line) or without (dashed line) 0.5 mg mL^{-1} SWCNT. Laccase concentration is 1 mg mL^{-1}. Light path length is 0.02 cm. Bottom: Difference IR spectrum of the dried laccase film. Red square shows the Amide I band region with inset showing Gaussian band fitting.

at 218 nm mainly contributed by β-sheets demonstrated the essential antiparallel β-barrel structure that accommodates coppers in native laccase. Spectra comparison to existed reference set[69] suggested that native hydrated laccase contained 38.7% β-sheets, 6.8% α-helices and 54.5% unordered structures. In the presence of 20% ethanol, secondary composition of laccase changed slightly to 39.5% β-sheets, 7.7% α-helices and 54.5% unordered structures, showing that ethanol at a moderate concentration placed a negligible impact on laccase conformation. Addition of SWCNT altered the hydrophobicity of the surrounding environment of laccase in solution and resulted in blue shifts of both positive and negative peaks. A significant transition from β-sheets (36.7%) to α-helices (9.3%) was due to a protein domain deformation at the SWCNT-laccase interface. A dramatically larger transition (32.4% β-sheets and 14.9% α-helices) was observed when both SWCNTs and ethanol were present in solution, indicating an aggravated shape distortion of the β-barrel in laccase. These data demonstrate that ethanol molecules promote the hydrophobic

DOI: 10.1021/jacs.6b11469
J. Am. Chem. Soc. 2017, 139, 1565−1574

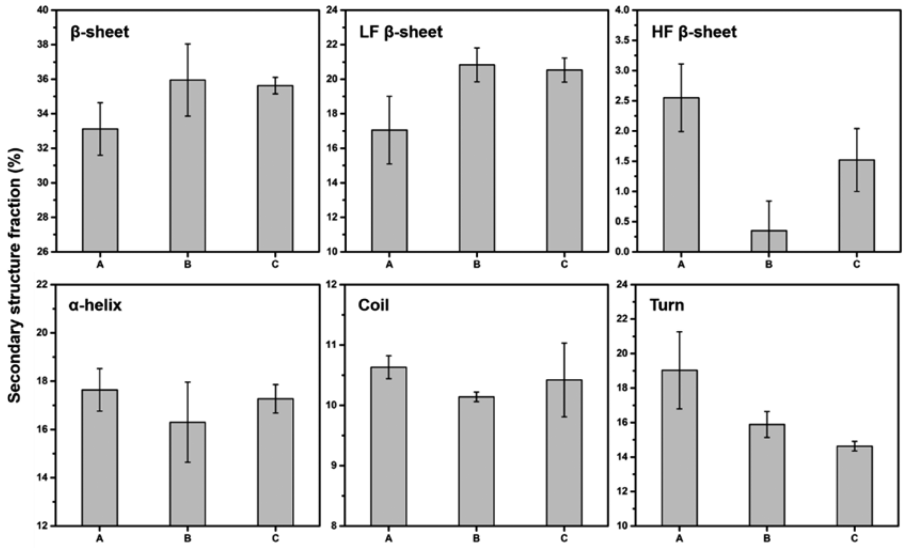

Figure 5. Fractions of different secondary structures in immobilized laccase: (A) laccase film; (B) untreated laccase-SWCNT film; (C) ethanol-treated laccase-SWCNT film. Error bars represent standard deviations of three independent measurements. LF and HF respectively stand for low-frequency and high-frequency.

interactions between SWCNTs and laccase, leading to partial denaturing that appear trivial in the absence of SWCNTs.

Conformation of adsorbed laccase on SWCNT surface in dry state was probed by ATR-IR. A typical difference IR spectrum of the laccase film is shown in Figure 4 (bottom). The peak in Amide I region (1700−1600 cm^{-1}) centered at ~1631 cm^{-1} is a characteristic of C═O stretch in protein backbone, frequency of which is very sensitive to secondary structures. Due to extensive overlapping in Amide I band, second- and fourth-derivative spectra were used to solve convoluted peaks (Figure S5). In combination with previously summarized peak positions,[81] six types of secondary structures were resolved to give 14 component peaks and relative contributions: β-sheets (1627 ± 2, 1635 ± 5 and 1642 ± 1 cm^{-1}), α-helices (1656 ± 2 cm^{-1}), random coils (1648 ± 3 cm^{-1}), turns (1667 ± 1, 1675 ± 1, 1680 ± 2 and 1685 ± 2 cm^{-1}), low-frequency (LF) β-sheets (1606 ± 2, 1615 ± 2 and 1622 ± 2 cm^{-1}) and high-frequency (HF) β-sheets (1691 ± 2 cm^{-1}), shown in Figure 5.

Compared to laccase deposited on a planar surface (the CaF_2 slide), laccase adsorbed on SWCNTs turned out to have more β-sheet content and a merely unaltered alpha content, which contrasts with the conformation transition trend observed in solution. Maintain of the ordered barrel structure implies that SWCNTs with high surface curvature help stabilize dehydrated laccase in its near-native form. Unexpectedly, the β-sheet fraction showed no distinction with and without ethanol involvement during immobilization. Although dissolved laccase underwent a partial denaturing/unfolding induced by SWCNTs and ethanol in solution, such a change faded with solvent evaporation. IR peaks at low frequencies (<1624 cm^{-1}) usually arise from protein−protein interaction-induced deformation. A larger contribution of these peaks to the overall band shape suggests more deformed β-sheets in laccase immobilized on SWCNTs than those in the laccase film. It is probably a result of protein aggregates or dense protein layers on SWCNT surfaces. No obvious impact of ethanol on protein deformation was observed in terms of almost the same LF β-sheet contents in adsorbed untreated or ethanol-treated laccase. In contrast, HF β-sheet corresponding to flexible β-extend was significantly affected by ethanol during enzyme immobilization, even though this type of structure only occupies a small fraction of the enzyme entity (Figure 1, highlighted in cyan). Its peak area ratio dropped just above zero after immobilization on SWCNTs, while increased by about 200% in ethanol-treated laccase. For unordered structures, ethanol did not alter the coil fraction but caused a significant loss of turns.

Effect of Ethanol on Orientation of the Immobilized Laccase. Like the C═O stretch in the peptide linkage, N−H in-plane bending gives rise to another characteristic Amide II band centered between 1600 and 1500 cm^{-1}. A larger Amide II peak was obtained with ethanol-treated laccase-SWCNT film, showing an increased amount of detectable N−H in-plane bending events. In fact, C═O stretch and N−H bending are perpendicular to each other in the plane of β-sheet and sensitive to its orientation with respect to the surface. Therefore, the relative change of Amide I and II band intensity is considered as a qualitative indicator of the protein orientation on surface, and we used the Amide I/II ratio to assess the orientation of immobilized laccase on SWCNT surface.[82−85] As shown in Figure 6, the Amide I/II ratio was effectively reduced by ethanol, indicating a significant change of the laccase orientation.

There are two types of orientation that can be adopted by a β-strand on the surface of SWCNTs, "flat-on" and "end-on". In the "flat-on" orientation, both vibration motions of C═O and N−H are parallel to the surface. In the "end-on" orientation, the N−H in-plane bending switches to a perpendicular direction with respect to the surface. As a result, its vibration intensity detected by ATR-IR increases.[85] Our data suggests a trend that the relative orientation of β-sheets was converted from "flat-on" to "end-on" under the influence of ethanol.

Besides the relative Amide I/II peak intensity ratio, fraction change of HF β-sheets and unordered structures is another useful hint for drawing the picture. As told by resolved component IR bands, an increase of detectable C═O stretch motions in HF β-sheets indicates a similar conversion of the flexible β-extends from the "flat-on" to "end-on" orientation, which was associated with loss of turns. Taken together with the crystal structure of laccase, in which the flexible β-extends and turns are guarding the binding pocket opening (Figure 1),

DOI: 10.1021/jacs.6b11469
J. Am. Chem. Soc. 2017, 139, 1565−1574

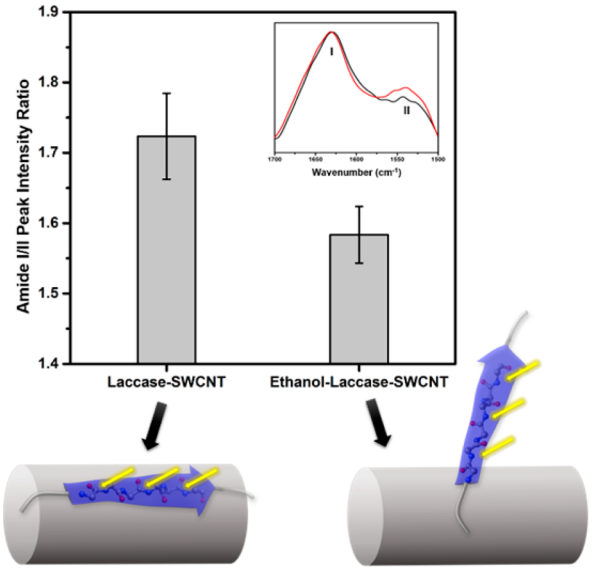

Figure 6. Two orientations of β-strand at the surface of SWCNT predicted from the Amide I/II peak intensity ratios. Inset: Amide I and II band regions on difference IR spectra (corrected by a linear baseline between 1700 and 1500 cm^{-1}) of the untreated laccase-SWCNT film (black line) and ethanol-treated laccase-SWCNT film (red line). Yellow arrows represent incident light. Amide bonds (ball and sticks) are in the plane of β-strand.

an "end-on" position of laccase with its pocket facing toward the CNT sidewall is the most plausible choice in this particular case.

Effect of Other Organic Solvents on the Immobilized Laccase. As a step forward from our results with ethanol, we investigated effects of more organic solvents on laccase immobilization. Figure 7 displays a set of cyclic voltammograms recorded with laccase electrodes prepared with acetone, acetonitrile (ACN), DMF or DMSO. Maximum reductive

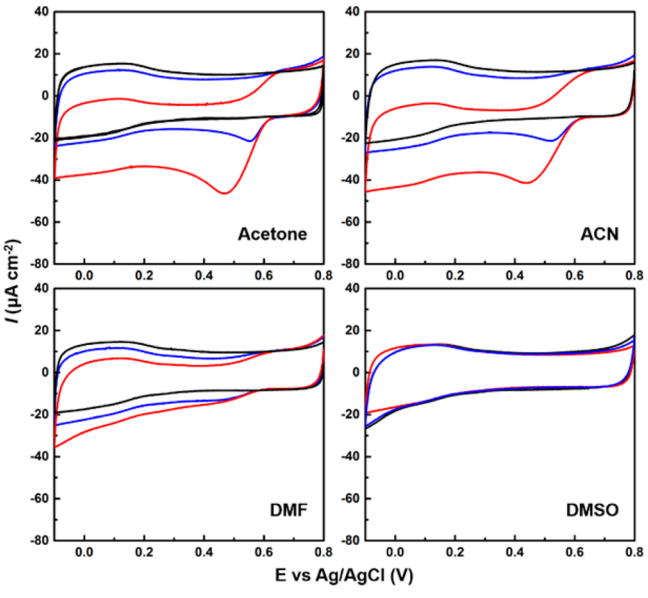

Figure 7. Cyclic voltammograms of laccase-modified SWCNT/GCE prepared with other organic solvents in N_2-saturated (black line), air-saturated (blue line) and O_2-saturated (red line) sodium phosphate buffer (0.1 M, pH 6.0). Scan rate, 10 mV sec^{-1}.

current densities of acetone- and ACN-treated electrodes in oxygenated solution were significantly increased respectively by approximately 400% and 350%, as compared to that of the untreated laccase electrode. DMF treatment brought down the oxygen responsive current densities, which completely went away after DMSO.

As displayed in Figure 8, there seems to be a tendency that current enhancement decreases as the change of β-barrels holding copper sites is intensified. With respect to untreated laccase on SWCNTs, the fraction of regular β-sheets is similar in acetone-treated laccase but altered significantly in ACN-, DMF- and DMSO-treated laccase. Thus, reduction in direct bioelectrocatalytic performance of corresponding electrodes follows the order of DMSO > DMF > ACN > acetone. The fractions of LF β-sheets in DMF- and DMSO-treated laccase also dramatically increase, implying much higher degree of deformation of β-barrels, while in the HF β-sheet region, fraction change is somehow ruleless. Alpha and turn contents are in no statistical differences upon organic solvent treatment, except that DMF converted merely half of α-helices and turns to β-sheets (especially deformed β-sheets). Random coil contents in acetone and ACN-treated laccase are increased by about 30%, most likely due to further unfolding of deformed β-sheets.

Discussion. Laccase catalyzes the oxidation of a broad range of aromatic (mostly phenolic) compounds, suggesting a promiscuous binding pocket other than a specific binding site (Figure 1). Substrate accommodation mainly relies on $\pi-\pi$ interactions and hydrogen bonding with residues in the pocket. As a matter of fact, all available binding sites are close to the enzyme surface and easily accessed by solvent molecules. Adverse impacts on laccase activity imposed by organic solvents in a homogeneous aqueous-nonaqueous mixture follow the formation of new hydrogen bonds (inhibition effect) and globule distortion by water substitution in the hydration shell (denaturing effect).[86] Standing on this basis, we initially proposed that partial unfolding of laccase under denaturing effect to reduce the spatial hindrance between buried copper sites and surfaces of CNTs was responsible for observed improvement of current response in direct bioelectrocatalysis by ethanol-aided laccase immobilization. However, CD and IR data provided opposing evidence. Ethanol at 20% did not induce significant conformation alteration in a homogeneous solution, whereas just intensified a reversible distortion of the β-barrel at the enzyme-CNT interface. This finding is in accordance with studies by Mozhaev et al. and Rodakiewicz-Nowak et al. that have demonstrated the prevailing of inhibition effect over denaturing effect of organic solvents at moderate concentrations.[73,74,86] Therefore, instead of driving laccase to unfold, ethanol promoted contact of laccase and the CNT surface to facilitate a favorable "end-on" orientation (Figure 9). For laccase, ethanol behaved as a weak mixed competitive inhibitor that partly substituted bound water molecules in the binding pocket by forming new hydrogen bonds. For SWCNTs, readily adsorbed ethanol molecules wetted the hydrophobic surfaces, turning them more amenable to ethanol-substituted laccase from the aqueous phase. The stability (over time) of SWCNT dispersion against agglomeration and precipitation in solution followed the order of ethanol-laccase-SWCNT > laccase-SWCNT ≈ ethanol-SWCNT > SWCNT (results not shown). In this sense, surface wetting by organic solvent molecules played an essential part in establish-

DOI: 10.1021/jacs.6b11469
J. Am. Chem. Soc. 2017, 139, 1565−1574

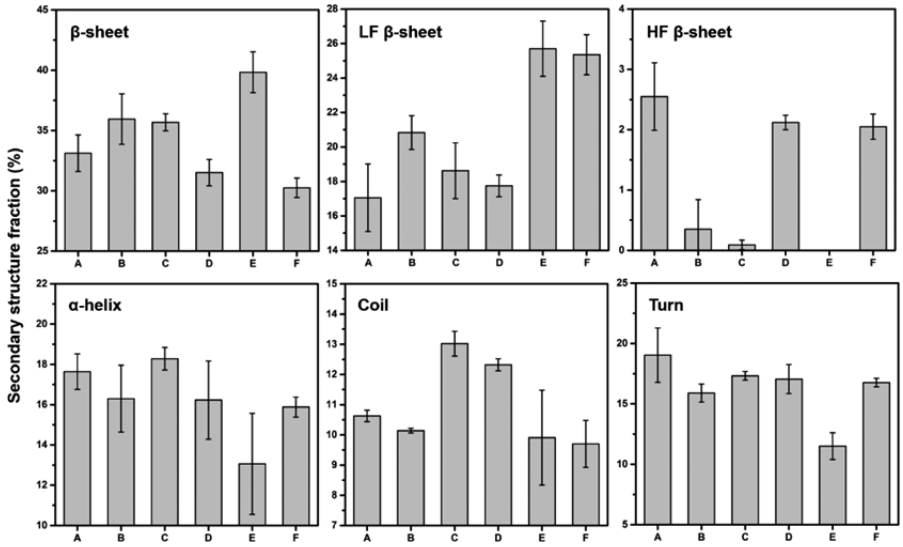

Figure 8. Fractions of different secondary structures in immobilized laccase: (A) laccase film; (B) untreated laccase-SWCNT film; (C) acetone-treated laccase-SWCNT film; (D) ACN-treated laccase-SWCNT film; (E) DMF-treated laccase-SWCNT film; (F) DMSO-treated laccase-SWCNT film. Error bars represent standard deviations of three independent measurements.

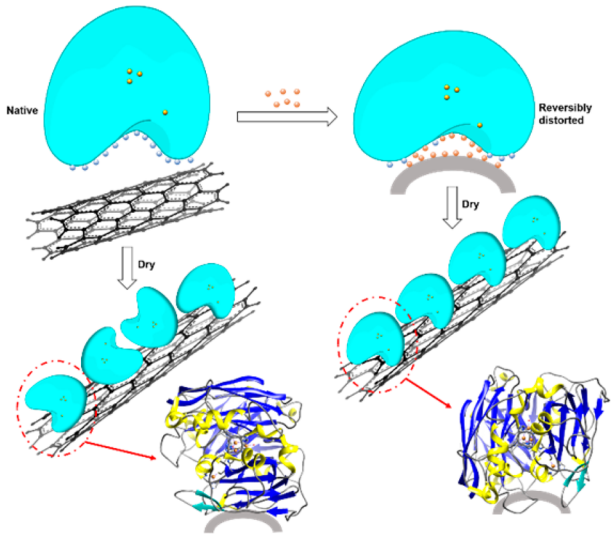

Figure 9. Schematic illustration of the effect of ethanol on the orientation of laccase on SWCNT. Orange spheres represent the copper ions. Light blue and pink spheres respectively represent the water and ethanol molecules in the hydration shell of laccase.

ing sufficient heterogeneous contact, more or less similar to surfactant-assisted DET on CNTs.[87]

It should be admitted that cyclic voltammetric and spectroscopic data presented here only give averaged results over the whole laccase population. Idealizing each single laccase molecule orientation simply by physical adsorption is not easy. In other words, different orientations existed on either untreated laccase-SWCNT or ethanol-treated laccase-SWCNT electrode. Laccase molecules in the absence of ethanol were immobilized in a more random fashion during electrode deposition, while ethanol-wetted interface was evidenced to provide increased population or probability of laccase adopting the beneficial orientation (Figure 9). One indirect proof of this mechanism comes from the cathodic current contribution at more negative potentials, assigned to direct electroreduction of T2/T3 coppers in closer proximity with SWCNT surfaces. Compared to DET at T1 copper, longer tunneling distance between the electrode and T2/T3 copper cluster (over at least 1.2 nm) would yield lower electron transfer rate, so DET at T2/T3 copper cluster was barely achieved except for a limited number of studies about wiring the T2/T3 site on gold surfaces with the substrate binding pocket facing outward.[15,60,88] The observed cathodic current independent of Cl^- binding but suppressed by F^- began to emerge at +0.40 V, which is to some extent consistent with reported larger overpotentials for T2/T3 DET process.[15,60] However, this indeed needs more experimental evidence as it has never been investigated on carbonaceous electrodes.

Notably, enhancement of the maximum oxygen reduction current density upon ethanol treatment was obviously larger under hydrostatic condition (ca. 600%, Figure 2B) than that under hydrodynamic condition (ca. 70%, Figure 2C). Control test by examining ethanol-wetted SWCNT electrodes in 0.1 M phosphate buffer (pH 6.0) containing 1 mM $K_3Fe(CN)_6$ found that the change in CV was negligible (Figure S6). Traces of ethanol molecules adsorbed on SWCNT surfaces did not alter either the dynamic behavior of water-soluble species (such as dissolved oxygen molecules) within the hydrophobic matrix or the conductivity and solvent-accessible surface area of the SWCNT-modified electrode. This then brought up another interesting question: was there an easier access of oxygen molecules to T2/T3 copper cluster embedded in the ethanol-treated laccase? Although secondary structure analysis has excluded an exposure of T2/T3 cluster to the solution, subtle local protein domain changes induced by bound ethanol could not be completely ruled out. Second-derivative IR spectra demonstrate a partial substitution of bound water molecules by ethanol molecules in terms of upward shifts of C═O stretch frequencies due to weaker H-bonds (Figure S7).[89] Particularly, band positions (1800−1700 cm^{-1}) related to C═O stretch in aspartate and glutamate residues constituting the solvent channel to T2 copper[1,90] have all shifted 2−3 cm^{-1} up, indicating that its inner hydrophilic "wall" was decorated with ethanol molecules. Transport of hydrophobic oxygen molecules to the reduction site might be facilitated through the ethanol-

DOI: 10.1021/jacs.6b11469
J. Am. Chem. Soc. 2017, 139, 1565−1574

substituted solvent channel, which merits our in-depth research attention.

With more organic solvents investigated, we found it difficult to extract a universal rule in regulating direct bioelectrocatalysis by laccase. However, there is no doubt that a trade-off between surface wetting and denaturing effect affects the performance of the as-prepared electrodes. As the polarity of organic solvents reduces (Table S1), its capability of joining hydrohpbilic enzymes and hydrohpobic SWCNTs increases, and the resultant catalytic current heightens in the order of DMSO < DMF < ACN < acetone < ethanol. Interestingly, distortion of the globular protein shape is aggravated in a reversed trend, contrary to our statement that promoted SWCNT-laccase contact induces higher degree of reversible unfolding. To explain such a discrepancy, further inspection of the physiochemical properties showed that organic solvents with both higher denaturing capacity (proposed by Khmelnitsky et al.)[91] and lower vapor pressure intended to exert stronger and extended denaturing effect on laccase during solvent evaporation, which diminished positive effects of surface wetting. This is especially in line with the current disappearance after DMF- or DMSO-aided immobilization. Compared to water (2.34 kPa, 20 °C), DMF (0.36 kPa, 20 °C) or DMSO (0.06 kPa, 20 °C) was gradually concentrated due to slower evaporation during enzyme immobilization and eventually deactivated laccase, thus releasing coordinated copper ions from completely unfolded enzymes. For ethanol (5.95 kPa, 20 °C), ACN (5.00 kPa, 20 °C) or acetone (24.5 kPa, 20 °C) with a higher vapor pressure, organic solvent accumulation was avoided. Even though acetone has the highest denaturing capacity, rapid evaporation might offset part of its denaturing effect on laccase conformation.

CONCLUSION

Interactions between proteins in solution and solid surfaces dominate the protein immobilization and determine the bioelectrocatalytic activities. A lot of material and protein engineering-based methods have been provided to the construction of the electrode-protein interfaces enabling efficient direct bioelectrocatalysis. In this work, we reexamine a simple immobilization strategy that effectively improves direct electrocatalytic current response by organic solvent-assisted immobilization of laccase on SWCNTs. After an in-depth exploration of the effects of water-miscible nonaqueous solvents on laccase immobilization from structural biological and physicochemical perspectives, we demonstrate the important role of surface wetting and protein denaturing in regulating enzyme conformation and orientation on the surfaces of SWCNTs. As suggested in the present study, organic solvents with lower polarity, weaker denaturing capcity and higher vapor pressure turn out to be well-suited for assisting DET. On the contrary, organic solvents with higher polarity, stronger denaturing capacity and lower vapor pressure disfavor the laccase-SWCNTs interactions and direct bioelectrocatalysis.

Turning back to the beginning question that whether and how organic solvents affect the subsequent enzymatic electrode performance, we can state that some knowledge has been gained toward understanding of contributing factors, especially surface wettability, in regulating laccase immobilization on hydrophobic surfaces of nanomaterials, even though our current knowledge is still distant from fully unravelling the underneath answer including a quantitative correlation between physiochemical properties of organic solvents and laccase DET efficiency. At this moment in time, we believe in the prominent future of water-miscible, nonpolar organic small molecules as useful tools in the design of electrode-enzyme interfaces on new tailor-made platforms, whose surface wettabilities can be fine-tuned or even patterned to achieve optimum, individualized enzyme immobilization.

ASSOCIATED CONTENT

Supporting Information

The Supporting Information is available free of charge on the ACS Publications website at DOI: 10.1021/jacs.6b11469.

SDS-PAGE, UV−vis characterization, polarization curves of laccase-SWCNT electrodes, cyclic voltammograms for control experiments, second-/fourth-derivative IR spectra showing component secondary structure peaks and band shifts, and physiochemical parameters of tested organic solvents (PDF)

AUTHOR INFORMATION

Corresponding Author

*lqmao@iccas.ac.cn

ORCID

Lanqun Mao: 0000-0001-8286-9321

Author Contributions

§F.W. and L.S. contributed equally.

Notes

The authors declare no competing financial interest.

ACKNOWLEDGMENTS

We acknowledge financial support from the National Natural Science Foundation of China (Grant No. 21321003, 21435007, and 21210007 for L. Mao, 21322503 and 21475138 for P. Yu), and National Key Research Development Project of China (2016YFA0200104, 2013CB933704), China Postdoctoral Science Foundation and the Chinese Academy of Sciences.

REFERENCES

(1) Piontek, K.; Antorini, M.; Choinowski, T. *J. Biol. Chem.* **2002**, *277*, 37663−37669.

(2) Cosnier, S.; Holzinger, M.; Goff, A. L. *Front. Bioeng. Biotechnol.* **2014**, *2*, 1−6.

(3) Page, C. C.; Moser, C. C.; Chen, X.; Dutton, P. L. *Nature* **1999**, *402*, 47−52.

(4) Voityuk, A. A. *J. Phys. Chem. B* **2011**, *115*, 12202−12207.

(5) Berezin, I. V.; Bogdanovskaya, V. A.; Tarasevich, M. R.; Varfolomeev, S. D.; Yaropolov, A. I. *Doklady Akad. Nauk SSSR* **1978**, *240*, 615−619.

(6) Yaropolov, A. I.; Kharybin, A. N.; Emnéus, J.; Marko-Varga, G.; Gorton, L. *Bioelectrochem. Bioenerg.* **1996**, *40*, 49−57.

(7) Zhao, J.; Henkens, R. W.; Stonehuerner, J.; O'Daly, J. P.; Crumbliss, A. L. *J. Electroanal. Chem.* **1992**, *327*, 109−119.

(8) Tarasevich, M. R.; Bogdanovskaya, V. A.; Kuznetsova, L. N. *Russ. J. Electrochem.* **2001**, *37*, 833−837.

(9) Tarasevich, M. R.; Bogdanovskaya, V. A.; Kapustin, A. V. *Electrochem. Commun.* **2003**, *5*, 491−496.

(10) Bogdanovskaya, V. A.; Gavrilova, E. F.; Tarasevich, M. R. *Soviet Electrochem.* **1986**, *22*, 697−701.

(11) Tarasevich, M. R.; Yaropolov, A. I.; Bogdanovskaya, V. A.; Varfolomeev, S. D. *Bioelectrochem. Bioenerg.* **1979**, *6*, 393−403.

(12) Lee, C. W.; Gray, H. B.; Anson, F. C.; Malmstrom, B. G. *J. Electroanal. Chem. Interfacial Electrochem.* **1984**, *172*, 289−300.

(13) Thuesen, M. H.; Farver, O.; Reinhammar, B.; Ulstrup, J. *Acta Chem. Scand.* **1998**, *52*, 555−562.

DOI: 10.1021/jacs.6b11469
J. Am. Chem. Soc. 2017, 139, 1565−1574

(14) Shleev, S.; Jarosz-Wilkolazka, A.; Khalunina, A.; Morozova, O.; Yaropolov, A.; Ruzgas, T.; Gorton, L. *Bioelectrochemistry* **2005**, *67*, 115−127.
(15) Shleev, S.; Christenson, A.; Serezhenkov, V.; Burbaev, D.; Yaropolov, A.; Gorton, L.; Ruzgas, T. *Biochem. J.* **2005**, *385*, 745−754.
(16) Qiu, H.; Xu, C.; Huang, X.; Ding, Y.; Qu, Y.; Gao, P. *J. Phys. Chem. C* **2008**, *112*, 14781−14785.
(17) Rubenwolf, S.; Strohmeier, O.; Kloke, A.; Kerzenmachera, S.; Zengerle, R.; Stetten, F. v. *Biosens. Bioelectron.* **2010**, *26*, 841−845.
(18) Salaj-Kosla, U.; Pöller, S.; Schuhmann, W.; Shleev, S.; Magner, E. *Bioelectrochemistry* **2013**, *91*, 15−20.
(19) Majdecka, D.; Bilewicz, R. *J. Solid State Electrochem.* **2016**, *20*, 949−955.
(20) Stolarczyk, K.; Nazaruk, E.; Rogalski, J.; Bilewicz, R. *Electrochim. Acta* **2008**, *53*, 3983−3990.
(21) Yan, Y.; Zheng, W.; Su, L.; Mao, L. *Adv. Mater.* **2006**, *18*, 2639−2643.
(22) Zheng, W.; Li, Q.; Su, L.; Yan, Y.; Zhang, J.; Mao, L. *Electroanalysis* **2006**, *18*, 587−594.
(23) Rahman, M. A.; Noh, H.-B.; Shim, Y.-B. *Anal. Chem.* **2008**, *80*, 8020−8027.
(24) Zheng, W.; Zhou, H. M.; Zheng, Y. F.; Wang, N. *Chem. Phys. Lett.* **2008**, *457*, 381−385.
(25) Deng, L.; Shang, L.; Wang, Y.; Wang, T.; Chen, H.; Dong, S. *Electrochem. Commun.* **2008**, *10*, 1012−1015.
(26) Shleev, S.; Shumakovich, G.; Morozova, O.; Yaropolov, A. *Fuel Cells* **2009**, *10*, 726−733.
(27) Krikstolaityte, V.; Barrantes, A.; Ramanavicius, A.; Arnebrant, T.; Shleev, S.; Ruzgas, T. *Bioelectrochemistry* **2014**, *95*, 1−6.
(28) Dagys, M.; Haberska, K.; Shleev, S.; Arnebrant, T.; Kulys, J.; Ruzgas, T. *Electrochem. Commun.* **2010**, *12*, 933−935.
(29) Gutiérrez-Sánchez, C.; Pita, M.; Vaz-Domínguez, C.; Shleev, S.; Lacey, A. L. D. *J. Am. Chem. Soc.* **2012**, *134*, 17212−17220.
(30) Gutiérrez-Sánchez, C.; Jia, W.; Beyl, Y.; Pita, M.; Schuhmann, W.; Lacey, A. L. D.; Stoica, L. *Electrochim. Acta* **2012**, *82*, 218−223.
(31) Brondani, D.; Souza, B. d.; Souza, B. S.; Neves, A.; Vieira, I. C. *Biosens. Bioelectron.* **2013**, *42*, 242−247.
(32) Santucci, R.; Ferri, T.; Morpurgo, L.; Savini, I.; Avigliano, L. *Biochem. J.* **1998**, *332*, 611−615.
(33) Bogdanovskaya, V. A.; Tarasevich, M. R.; Kuznetsova, L. N.; Reznik, M. F.; Kasatkin, E. V. *Biosens. Bioelectron.* **2002**, *17*, 945−951.
(34) Karyakin, A. A.; Karyakina, E. E.; Gorton, L. *Anal. Chem.* **1996**, *68*, 4335−4341.
(35) Nazaruk, E.; Michota, A.; Bukowska, J.; Shleev, S.; Gorton, L.; Bilewicz, R. *JBIC, J. Biol. Inorg. Chem.* **2007**, *12*, 335−344.
(36) Kamitaka, Y.; Tsujimura, S.; Setoyama, N.; Kajino, T.; Kano, K. *Phys. Chem. Chem. Phys.* **2007**, *9*, 1793−1801.
(37) Stolarczyk, K.; Nazaruk, E.; Rogalski, J.; Bilewicz, R. *Electrochem. Commun.* **2007**, *9*, 115−118.
(38) Gellett, W.; Schumacher, J.; Kesmez, M.; Le, D.; Minteer, S. D. *J. Electrochem. Soc.* **2010**, *157*, B557−B562.
(39) Gupta, G.; Rajendran, V.; Atanassov, P. *Electroanalysis* **2004**, *16*, 13−14.
(40) Kuznetsov, B. A.; Shumakovich, G. P.; Koroleva, O. V.; Yaropolov, A. I. *Biosens. Bioelectron.* **2001**, *16*, 73−84.
(41) Hyung, K. H.; Jun, K. Y.; Hong, H.-G.; Kin, H. S.; Shin, W. *Bull. Korean Chem. Soc.* **1997**, *18*, 564−566.
(42) Vaz-Dominguez, C.; Campuzano, S.; Rüdiger, O.; Gorbacheva, M. P. M.; Shleev, S.; Fernandez, V. M.; Lacey, A. L. D. *Biosens. Bioelectron.* **2008**, *24*, 531−537.
(43) Martinez-Ortiz, J.; Flores, R.; Vazquez-Duhalt, R. *Biosens. Bioelectron.* **2011**, *26*, 2626−2631.
(44) Olejnik, P.; Palys, B.; Kowalczyk, A.; Nowicka, A. M. *J. Phys. Chem. C* **2012**, *116*, 25911−25918.
(45) Giroud, F.; Minteer, S. D. *Electrochem. Commun.* **2013**, *34*, 157−160.
(46) Zhou, X.-h.; Huang, X.-r.; Liu, L.-h.; Bai, X.; Shi, H.-c. *RSC Adv.* **2013**, *3*, 18036−18043.
(47) Hou, C.; Yang, D.; Liang, B.; Li, A. *Anal. Chem.* **2014**, *86*, 6057−6063.
(48) Nazaruk, E.; Karaskiewicz, M.; Żelechowska, K.; Biernat, J. F.; Rogalski, J.; Bilewicz, R. *Electrochem. Commun.* **2012**, *14*, 67−70.
(49) Blanford, C. F.; Heath, R. S.; Armstrong, F. A. *Chem. Commun.* **2007**, *2007*, 1710−1712.
(50) Blanford, C. F.; Foster, C. E.; Heath, R. S.; Armstrong, F. A. *Faraday Discuss.* **2008**, *140*, 319−335.
(51) Thorum, M. S.; Anderson, C. A.; Hatch, J. J.; Campbell, A. S.; Marshall, N. M.; Zimmerman, S. C.; Lu, Y.; Gewirth, A. A. *J. Phys. Chem. Lett.* **2010**, *1*, 2251−2254.
(52) Sosna, M.; tien, J.-M. C.; Kilburn, J. D.; Bartlett, P. N. *Phys. Chem. Chem. Phys.* **2010**, *12*, 10018−10026.
(53) Meredith, M. T.; Minson, M.; Hickey, D.; Artyushkova, K.; Glatzhofer, D. T.; Minteer, S. D. *ACS Catal.* **2011**, *1*, 1683−1690.
(54) Lalaoui, N. m.; David, R.; Jamet, H. l. n.; Holzinger, M.; Goff, A. L.; Cosnier, S. *ACS Catal.* **2016**, *6*, 4259−4264.
(55) Holzinger, M.; Bouffier, L.; Vilialonga, R.; Cosnier, S. *Biosens. Bioelectron.* **2009**, *24*, 1128−1134.
(56) Stolarczyk, K.; Łyp, D.; Żelechowska, K.; Biernat, J. F.; Rogalski, J.; Bilewicz, R. *Electrochim. Acta* **2012**, *79*, 74−81.
(57) Stolarczyk, K.; Sepelowska, M.; Lyp, D.; Zelechowska, K.; Biernat, J. F.; Rogalski, J.; Farmer, K. D.; Roberts, K. N.; Bilewicz, R. *Bioelectrochemistry* **2012**, *87*, 154−163.
(58) Lalaoui, N.; Elouarzaki, K.; Le Goff, A.; Holzinger, M.; Cosnier, S. *Chem. Commun.* **2013**, *49*, 9281−9283.
(59) Tsujimura, S.; Asahi, M.; Goda-Tsutsumi, M.; Shirai, O.; Kano, K.; Miyazaki, K. *Phys. Chem. Chem. Phys.* **2013**, *15*, 20585−20589.
(60) Li, Y.; Zhang, J.; Huanga, X.; Wang, T. *Biochem. Biophys. Res. Commun.* **2014**, *446*, 201−205.
(61) Gelo-Pujic, M.; Kim, H.-H.; Butlin, N. G.; Palmore, G. T. R. *Appl. Environ. Microbiol.* **1999**, *65*, 5515−5521.
(62) Gallaway, J.; Wheeldon, I.; Rincon, R.; Atanassov, P.; Banta, S.; Barton, S. C. *Biosens. Bioelectron.* **2008**, *23*, 1229−1235.
(63) Guan, D.; Kurra, Y.; Liu, W.; Chen, Z. *Chem. Commun.* **2015**, *51*, 2522−2525.
(64) Miyake, T.; Yoshino, S.; Yamada, T.; Hata, K.; Nishizawa, M. *J. Am. Chem. Soc.* **2011**, *133*, 5129−5134.
(65) Zebda, A.; Gondran, C.; Goff, A. L.; Holzinger, M.; Cinquin, P.; Cosnier, S. *Nat. Commun.* **2011**, *2*, 1−6.
(66) Parimi, N. S.; Umasankar, Y.; Atanassov, P.; Ramasamy, R. P. *ACS Catal.* **2012**, *2*, 38−44.
(67) Gu, Z.; Yang, Z.; Chong, Y.; Ge, C.; Weber, J. K.; Bell, D. R.; Zhou, R. *Sci. Rep.* **2015**, *5*, 10886−10894.
(68) Yaropolov, A.; Shleev, S.; Zaitseva, E.; Emnéus, J.; Marko-Varga, G.; Gorton, L. *Bioelectrochemistry* **2007**, *70*, 199−204.
(69) Sreerama, N.; Woody, R. W. *Anal. Biochem.* **2000**, *287*, 252−260.
(70) Lobley, A.; Whitmore, L.; Wallace, B. A. *Bioinformatics* **2002**, *18*, 211−212.
(71) Whitmore, L.; Wallace, B. A. *Biopolymers* **2008**, *89*, 392−400.
(72) Whitmore, L.; Wallace, B. A. *Nucleic Acids Res.* **2004**, *32*, W668−673.
(73) Rodakiewicz-Nowak, J.; Haber, J.; Pozdnyakova, N.; Leontievsky, A.; Golovleva, L. A. *Biosci. Rep.* **1999**, *19*, 589−600.
(74) Rodakiewicz-Nowak, J.; Kasture, S. M.; Dudek, B.; Haber, J. *J. Mol. Catal. B: Enzym.* **2000**, *11*, 1−11.
(75) Chen, W.; Duan, L.; Zhu, D. *Environ. Sci. Technol.* **2007**, *41*, 8295−8300.
(76) Christenson, A.; Dimcheva, N.; Ferapontova, E. E.; Gorton, L.; Ruzgas, T.; Stoica, L.; Shleev, S.; Yaropolov, A. I.; Haltrich, D.; Thorneley, R. N. F.; Austf, S. D. *Electroanalysis* **2004**, *16*, 1074−1092.
(77) Jones, S. M.; Solomon, E. I. *Cell. Mol. Life Sci.* **2015**, *72*, 869−883.
(78) Goff, A. L.; Holzinger, M.; Cosnier, S. *Cell. Mol. Life Sci.* **2015**, *72*, 941−952.
(79) Beyl, Y.; Guschin, D. A.; Shleev, S.; Schuhmann, W. *Electrochem. Commun.* **2011**, *13*, 474−476.

DOI: 10.1021/jacs.6b11469
J. Am. Chem. Soc. 2017, 139, 1565−1574

(80) Vaz-Dominguez, C.; Campuzano, S.; Rüdiger, O.; Pita, M.; Gorbacheva, M.; Shleev, S.; Fernandez, V. M.; Lacey, A. L. D. *Biosens. Bioelectron.* **2008**, *24*, 531−537.
(81) Kong, J.; Yu, S. *Acta Biochim. Biophys. Sin.* **2007**, *39*, 549−559.
(82) Lenk, T. J.; Horbett, T. A.; Ratner, B. D.; Chittur, K. K. *Langmuir* **1991**, *7*, 1755−1764.
(83) Roach, P.; Farrar, D.; Perry, C. C. *J. Am. Chem. Soc.* **2005**, *127*, 8168−8173.
(84) Roach, P.; Farrar, D.; Perry, C. C. *J. Am. Chem. Soc.* **2006**, *128*, 3939−3945.
(85) Olejnik, P.; Pawłowska, A.; Pałys, B. *Electrochim. Acta* **2013**, *110*, 105−111.
(86) Mozhaev, V. V.; Khmelnitsky, Y. L.; Belova, M. V. S. A. B.; Klyachko, N. L.; Levashov, A. V.; Martinek, K. *Eur. J. Biochem.* **1989**, *184*, 597−602.
(87) Ogawa, Y.; Yoshino, S.; Miyakeab, T.; Nishizawa, M. *Phys. Chem. Chem. Phys.* **2014**, *16*, 13059−13062.
(88) Dagys, M.; Laurynėnas, A.; Ratautas, D.; Kulys, J.; Vidžiūnaitė, R.; Talaikis, M.; Niaura, G.; Marcinkevičienė, L.; Meškys, R.; Shleev, S. *Energy Environ. Sci.* **2017**, DOI: 10.1039/C6EE02232D.
(89) Barth, A. *Prog. Biophys. Mol. Biol.* **2000**, *74*, 141−173.
(90) Lyashenko, A. V.; Zhukova, Y. N.; Zhukhlistova, N. E.; Zaitsev, V. N.; Stepanova, E. V.; Kachalova, G. S.; Koroleva, O. V.; Voelter, W.; Betzel, C.; Tishkov, V. I.; Bento, I.; Gabdulkhakov, A. G.; Morgunova, E. Y.; Lindley, P. F.; Mikhailov, A. M. *Crystallogr. Rep.* **2006**, *51*, 817−823.
(91) Khmelnitsky, Y. L.; Mozhaev, V. V.; Belova, A. B.; Sergeeva, M. V.; Martinek, K. *Eur. J. Biochem.* **1991**, *198*, 31−41.

DOI: 10.1021/jacs.6b11469
J. Am. Chem. Soc. 2017, 139, 1565−1574